Water Supply

IWA PUBLISHING



Water Supply Vol 22 No 3, 2644 doi: 10.2166/ws.2021.445

# Hydrochemical characteristics, hydraulic connectivity and water quality assessment of multilayer aquifers in Western Suzhou City, Northern Anhui Province, China

Jie Ma [a,b,c,*], Song Chen[a,b,c], Songbao Feng[a,b,c] and Diandian Ding[a,b,c]

[a] School of Resources and Civil Engineering, Suzhou University, Suzhou, Anhui, China
[b] Key Laboratory of Mine Water Resource Utilization of Anhui Higher Education Institute, Suzhou University, Suzhou, Anhui, China
[c] National Engineering Research Center of Coal Mine Water Hazard Controlling, Suzhou, Anhui, China
*Corresponding author. E-mail: ahszumajie@163.com

JM, 0000-0002-7693-6038

## ABSTRACT

The present study focuses on the shallow phreatic aquifer (SA) and the upper confined aquifer (CA) developed in Cenozoic loose strata, which are the major regional groundwater resources for drinking, irrigation, industry and other water-related activities. Seven samples from SA and seventeen samples from CA were analyzed to depict the hydrochemical characteristics, categorize the hydrochemical facies, evaluate the hydraulic connectivity, and appraise the drinking water and irrigation water quality. The abundance of cations is $Na^+ > Ca^{2+} > Mg^{2+} > K^+$ and the anions is $HCO_3^- > SO_4^{2-} > Cl^-$ in both aquifers, respectively. Groundwater chemistry is controlled by water-rock interactions such as halite dissolution, ion exchange, reverse ion exchange, silicate weathering, and followed by the dissolution of Glauber's salt. The low connectivity and moderate connectivity between these two aquifers has engendered. The majority of the ion concentrations are within the limit for drinking, only one sample from the shallow aquifer was greater than the limit of 250 mg/L, a total of 29% from the shallow unconfined aquifer and 14% from the confined aquifer are not within the limit of 250 mg/L. The sodium absorption ratio (SAR), residual sodium carbonate (RSC) and soluble sodium percentage (%Na) values reveal that all the samples are appropriate for irrigation uses. The the US salinity laboratory (USSL) diagram shows that sixteen CA samples and all the SA samples fall in the C3S1 zone, implying high salinity hazard and low alkalinity hazard.

**Key words:** groundwater, hydraulic connectivity, hydrochemistry, isotope analysis, water quality assessment

## HIGHLIGHTS

- Hydrochemical characteristics and water-rock interactions were depicted.
- Connectivity index, stable isotope analysis, and cluster analysis were put forward to evaluate the hydraulic connectivity between the shallow phreatic aquifer and the upper confined aquifer developed in Cenozoic loose strata.
- The suitability for drinking and irrigation purposes was assessed, respectively.

## GRAPHICAL ABSTRACT

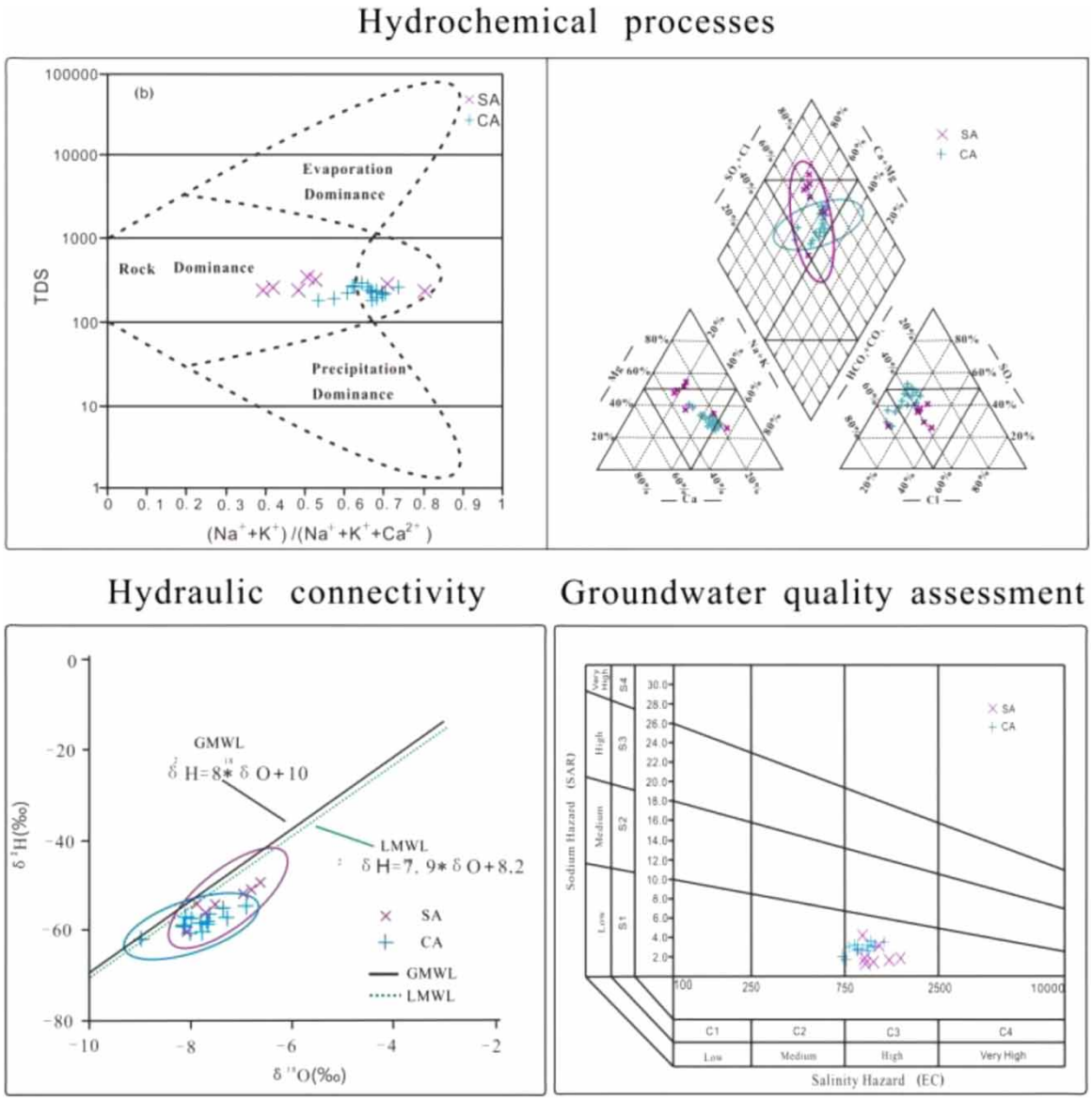


## INTRODUCTION

During the last several decades, the shallow groundwater aquifer has been exploited and utilized for domestic, agricultural and industrial supply, resulting in the remarkable decline of groundwater table, decrease of water yield, water quality degradation, and subsidence, etc. (Alkinani & Merkel 2017; Othman *et al.* 2018). In order to meet the increasing demands for clean, abundant, safety and pollution-free water, more and more profound groundwater aquifers with different depths have been taken as the high-quality water resources in many regions (Mengistu *et al.* 2019; Saha *et al.* 2020). Indeed, with the long-term groundwater extraction, aquifers separated by stable aquitards have generated the specific hydraulic connectivity, and the phenomenon of mutual seepage between aquifers has occurred. Therefore, to interpret the hydrochemical and hydraulic status between different groundwater aquifers, grasping the hydrochemical characteristics and hydraulic connectivity should be considered.

Owing to the complicated influence factors such as climate, landform, geology, and groundwater flow system, the extent and degree of the interaction between aquifers is very difficult to master (Li *et al.* 2016; Liu *et al.* 2019; Zaki *et al.* 2019).

The current hydrochemical compositions of the aquifers are the final manifestation during its formation process, which can be used to trace other hydrological information. Therefore, it is necessary to disclose groundwater compositions for appraising the hydrogeochemical evolution, hydraulic connectivity between different aquifers, and its suitability for various activities. Many scholars and experts have applied the integrated approaches to enable practical interpretation on hydrochemical processes by using the Piper diagram, ion ratios, isotope analysis, and multivariate statistical analysis (Mokadem *et al.* 2015; Ahmed *et al.* 2019; Islam *et al.* 2019; Zhang *et al.* 2019; Jayathunga *et al.* 2020). Numerous published literature have reported abundant and significant researches on the hydraulic connectivity between groundwater and surface water (King *et al.* 2014; Keshavarzi *et al.* 2017; Shakhane & Fourie 2019). Specially, a large number of studies have covered the hydraulic connectivity between different groundwater aquifers, with different lithology and formation ages, to identify the source of water-inrush in coal mines (Qian *et al.* 2016; Chen *et al.* 2019; Yang *et al.* 2020; Zhang *et al.* 2020).

In this study region, duo to the favorable sampling conditions such as surface water sampled on an embankment, a sandstone aquifer sampled on a mine roadway, and a limestone aquifer sampled on a hydrological borehole, an enormous amount of researches focused on a single aquifer such as Quaternary surface water, Carboniferous-Permian sandstone water and Carboniferous-Permian limestone water, have been conducted (Sun 2015; Sun & Gui 2015; Chen *et al.* 2019). However, with respect to groundwater of loose strata, along with the long-term groundwater extraction for several decades, water level depression, seepage between different groundwater aquifers, and fluctuation of groundwater quality have occurred, there are rare reports on the multi aquifers, especially to the shallow phreatic aquifer (SA) and the upper confined aquifer (CA) developed in the same geological period of Cenozoic loose strata. So, the objectives of this study were to (a) highlight the hydrochemical processes and water-rock interaction of these two aquifers, (b) evaluate the hydraulic connectivity between these two aquifers and (c) assess the groundwater quality of these two aquifers for drinking and irrigation purposes.

## STUDY AREA

### Location and climate

With 9,787 $km^2$ and appropriately 6.5827 million inhabitants (statistics up to 2019), Suzhou city is located in the center of Huaibei plain, Northern Anhui Province. The region lies within the north latitude 33°35′-33°40′ and east longitude 116° 50′-117°05′ (Figure 1). There are three typical geomorphic types, including plain, accounting for 91.0%, hills for 6.1%, and platform for 2.9%, respectively. The city has one municipal district and four counties, and the study area is situated in the west of the municipal district. This region experiences comfortable weather with a semi-humid monsoon climate, and is characterized by four distinctive seasons, ample sunlight, and moderate rainfall. The annual average temperature and precipitation are 14–15 °C and 774–896.3 mm, respectively.

### Geological and hydrogeological setting

In terms of the burial depth, recharge, runoff, drainage and groundwater yield, the aquifers can be divided into three water-bearing units separated by aquicludes, including the shallow phreatic aquifer, the upper confined aquifer, and the lower confined aquifer (Hu *et al.* 2014; Sun *et al.* 2016). The phreatic aquifer is chiefly comprised of fine sand mixed with medium sand and subsoil of the Holocene and Upper Pleistocene age, which is chiefly used for agriculture and domestic water. The upper confined aquifer mainly consists of fine alluvial sand, medium-coarse sand, locally mixed with gravel and sandy loam in the Middle Pleistocene and Lower Pleistocene segment, which is utilized as domestic water for local residents. The lower confined aquifer is chiefly represented by fine sand and medium sand with minor coarse sand, which belongs to the Neogene period and is regarded as reserved water resources. The shallow phreatic groundwater and the upper confined groundwater are the main water supply sources of the study area, with the thickness of water-bearing sand ranging from 20 m to 30 m, and the water yield of a single well can reach 1,000–2,000 $m^3$/d. According to the results from pumping tests, the hydraulic conductivity of the shallow phreatic groundwater and the upper confined groundwater is 30–280 $m^3$/d and 50–600 $m^3$/d, respectively.

Based on the calculation results of groundwater investigation statistics, long-term and large-scale groundwater exploitation with about 150 thousand $m^3$/d, accompanied by ground hardening preventing surface water infiltration, has led to a series of water environmental problems such as local over-exploitation of water resources, land subsidence and deterioration, etc. (Sun *et al.* 2016). In 2020, according to the monitoring data of the groundwater level conducted by the environmental agency, the shallow phreatic groundwater depth of the cone depression was 30.35 m, and the groundwater depth of the edge of cone depression was 2.25–4.46 m. For the upper confined groundwater, the groundwater depth of the cone depression was

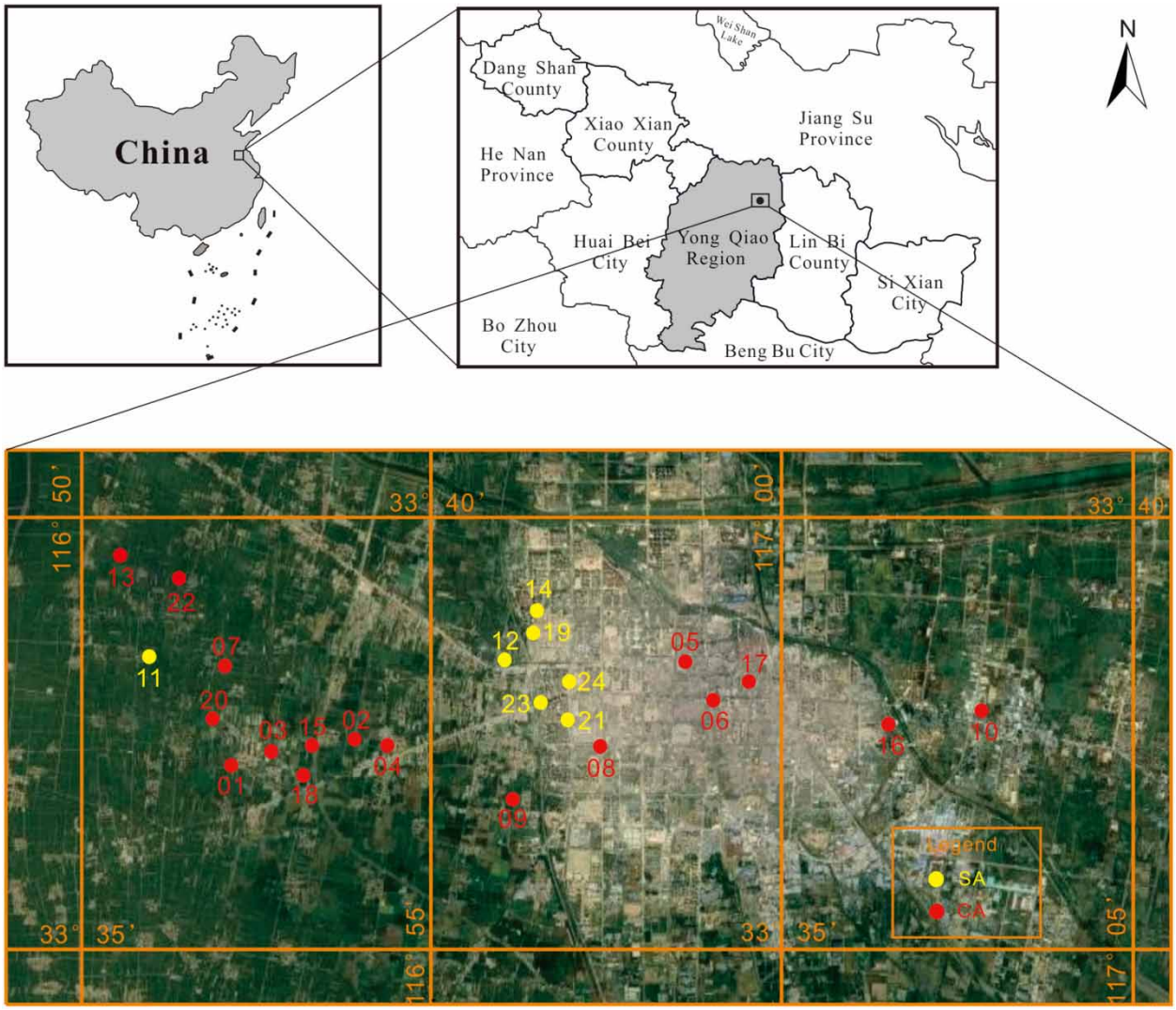


**Figure 1** | Location and sampling points of the study area.

28.30 m, and the groundwater depth of the edge of the cone depression was 5.04–7.01 m. Moreover, owing to long-term abstraction of the groundwater aquifers, hydraulic connectivity of these two aquifers has occurred under the water supply pressure.

## MATERIALS AND METHODS

### Sampling and laboratory analysis

In this study, the situ-sampling campaigns were performed in June and July 2018. Affected by population density, geographical location and hydrogeological conditions, the sampling sites were randomly arranged according to the existing water wells. Seventeen samples from CA with the depth of 80–120 m, and seven samples from SA with the depth of 12–40 m were taken, respectively. The phreatic aquifer samples, utilized for irrigation and individual domestic drinking, were collected from local residents' individual wells. The upper confined aquifer samples, used for urban drinking water supply, were obtained from the bore wells developed by the waterworks. Prior to sample collection, the wells were pumped for ten minutes. Sampling plastic polyethylene bottles were rinsed 3–5 times with the groundwater to be sampled to ensure the samples were pollution-free. During the sampling campain, the electrical conductivity (EC), the total dissolved solids (TDS) and pH were measured in situ using portable EC-, TDS-, and pH-meters, respectively. The sampling locations, which are shown in Figure 1, were recorded with GPS. One-L bottles were filled up at each sampling site. The hydrochemical analysis was conducted following

the standard procedures and methods for drinking water established by the Ministry of Environmental Protection of the People's Republic of China 2009 (Wu *et al.* 2015).

The concentrations of $Ca^{2+}$, $Mg^{2+}$, $Na^{+}$, $K^{+}$, $Cl^{-}$, $SO_4^{2-}$, and $HCO_3^{-}$ were measured in the National Engineering Research Center of Coal Mine Water Hazard Controlling, China. Major cations ($Ca^{2+}$, $Mg^{2+}$, $Na^{+}$, and $K^{+}$) were determined using the DIONEX-600 ion chromatography, and anions ($Cl^{-}$ and $SO_4^{2-}$) were analyzed by the DIONEX-900 ion chromatography, while $HCO_3^{-}$ concentration was analyzed by acid-base titration. All concentrations of the parameters are expressed in mg/L, except for pH and EC (μS/cm). To guarantee the validity and availability of hydrochemical analysis, charge balance error (CBE%) was computed after measurement. The CBE% values of all the samples are within $\pm 5\%$, which are allowed for the following analysis.

The isotope values of $\delta^2H$ and $\delta^{18}O$ were analyzed by liquid water isotope analyzer (LGR, LICA United technology Limited, CAN) in the Key Laboratory of Mine Water Resource Utilization of Anhui Higher Education Institute, Anhui Province, China. The isotopic compositions are reported with reference to V-SMOW (Vienna Standard Mean Ocean Water), and the precision was $\pm 0.1$ ‰ for $\delta^{18}O$ and $\pm 0.5$ ‰ for $\delta^2H$, respectively.

## Analytical methods

### Hydraulic connectivity analysis

Grasping the hydraulic connectivity of precipitation, surface water and groundwater is important to determine the recharge relationship, the hydrochemical interaction and the evolution processes between various water bodies. In order to understand the hydraulic connectivity between the shallow phreatic aquifer and the upper confined aquifer, cluster analysis, stable isotope analysis, and $Cl^{-}$ concentration as a connectivity index were conducted to master the groundwater connectivity between the two aquifers.

Q-type cluster analysis is a multivariate statistical method used to classify the samples into categories or groups by identifying their similar features and distinct features among different groups, the results of clustering analysis indicate that the samples in the same group exhibit the same properties (Qian *et al.* 2016; Chen *et al.* 2019; Zhang *et al.* 2020). In this study, the Ward method and Euclidean distance are conducted using SPSS. 19 to produce the dendrograms.

Hydrogen and oxygen isotopic compositions can be used to identify the replenishment and migration mechanism, and the mixing relationship (hydraulic connectivity) of different surface water and groundwaters (Zhang *et al.* 2020). Through comparison with the global meteoric water line (GMWL) and local meteoric water line (LMWL), it can been employed to obtain the isotope characteristics and the hydraulic connectivity of these two groundwater aquifers.

Similar hydrochemical characteristics should been observed when two adjacent aquifers are connected, and obvious different composition if disconnected (Li *et al.* 2018). In human activities-unaffected area, $Cl^{-}$ concentration is selected as an effective connectivity tracer to appraise the connectivity between two adjacent aquifers, which is calculated using Equation (1):

$$\text{Connectivity} = (Cl_1 - Cl_2)/1/2\,(Cl_1 + Cl_2) * 100\% \tag{1}$$

where $Cl_1$ and $Cl_2$ are the concentrations (mg/L) of the upper phreatic groundwater aquifer and the low confined groundwater aquifer, respectively. A value less than 0.2 indicates high connectivity, a value between 0.2 and 0.4 illustrates moderate connectivity, and a value more than 0.4 represents low connectivity (Li *et al.* 2018).

### Water quality assessment

Drinking water quality is evaluated through comparison with the limits of WHO 2011 (Table 1). The sodium adsorption ratio (SAR), residual sodium carbonate (RSC), soluble sodium percentage (%Na), and the US salinity laboratory (USSL) diagram are applied for the irrigation evaluation (Adimalla *et al.* 2018). The irrigation water quality assessment criteria based on SAR, RSC and %Na are shown in Table 4.

SAR represents the relationship between $Na^{+}$, $Ca^{2+}$ and $Mg^{2+}$, and it is calculated using Equation (2):

$$\text{SAR} = \frac{Na^{+}}{\sqrt{\frac{Ca^{2+} + Mg^{2+}}{2}}} \tag{2}$$

where, all cations are expressed in meq/L.

**Table 1** | Descriptive statistics of the physico-chemical parameters

| | | SA $n = 7$ | | | | CA $n = 17$ | | | |
|---|---|---|---|---|---|---|---|---|---|
| **Parameters** | **WHO** | **Min** | **Max** | **Mean** | **SD.** | **Min** | **Max** | **Mean** | **SD.** |
| $Na^+$ | 200.00 | 63.61 | 149.97 | 109.04 | 20.61 | 51.75 | 141.90 | 90.67 | 34.10 |
| $K^+$ | 12.00 | 0.56 | 1.19 | 0.88 | 0.16 | 0.55 | 0.77 | 0.66 | 0.08 |
| $Mg^{2+}$ | 150.00 | 25.15 | 42.38 | 35.51 | 4.92 | 34.63 | 88.12 | 59.68 | 21.54 |
| $Ca^{2+}$ | 200.00 | 40.60 | 73.17 | 51.02 | 9.85 | 30.62 | 79.62 | 62.37 | 17.43 |
| $Cl^-$ | 250.00 | 39.39 | 91.87 | 59.69 | 17.17 | 65.21 | 278.11 | 147.27 | 66.98 |
| $SO_4^{2-}$ | 250.00 | 90.73 | 355.41 | 213.37 | 75.40 | 117.37 | 262.56 | 196.92 | 49.94 |
| $HCO_3^-$ | – | 226.78 | 315.34 | 270.33 | 24.53 | 191.12 | 350.81 | 290.19 | 57.84 |
| pH | 6.5–8.5 | 7.30 | 7.80 | 7.51 | 0.15 | 7.30 | 7.70 | 7.51 | 0.14 |
| TDS | 1,000.00 | 181.00 | 299.00 | 232.41 | 33.87 | 235.00 | 353.00 | 279.29 | 45.12 |
| EC | – | 728.00 | 1,200.00 | 933.12 | 128.69 | 926.00 | 1,458.00 | 1,105.29 | 197.84 |

*Note*: all values are in mg/L, except pH, EC (μS/cm).

RSC represents the relationship between $HCO_3^-$, $CO_3^{2-}$, $Ca^{2+}$ and $Mg^{2+}$, and it is calculated using Equation (3):

$$RSC = (CO_3^{2-} + HCO_3^-) - (Ca^{2+} + Mg^{2+}) \quad (3)$$

where, all cations and anions are expressed in meq/L.

%Na represents the relationship between $K^+$, $Na^+$, $Ca^{2+}$ and $Mg^{2+}$, and it is calculated using Equation (4):

$$\%Na = \frac{Na^+}{Ca^{2+} + Mg^{2+} + Na^+ + K^+} \quad (4)$$

where, all cations are expressed in meq/L.

The USSL diagram consisted of EC and SAR. Based on EC, there are four salinity classes, including low salinity water (C1), medium salinity water (C2), high salinity water (C3), and very high salinity water (C4). According to SAR, there are four sodium (sodicity) classes, containing low sodium water (S1), medium sodium water (S2), high sodium water (S3), and very high sodium water (S4). The water can be divided into 16 categories. C1S1 is considered to be the most suitable for irrigation, and C4S4 is regarded as the worst.

## RESULTS AND DISCUSSION

### General hydrogeochemistry

To evaluate the hydrogeochemical variation of the major ions, the descriptive statistic results of physico-chemical parameters are presented in Table 1. For the upper confined aquifer, the pH values ranged from 7.30 to 7.80 with a mean of 7.51, showing the groundwater was neutral to light-alkalinity. The TDS ranged from 181.00 mg/L to 299.00 mg/L with an average value of 232.41 mg/L. All the samples were below the limit of 1,000 mg/L, indicating that the groundwater belonged to freshwater (Brindha *et al.* 2017). The values of $Na^+$, $K^+$, $Mg^{2+}$ and $Ca^{2+}$ varied from 63.61 mg/L to 149.97 mg/L, 0.56 mg/L to 1.19 mg/L, 25.15 mg/L to 42.38 mg/L and 40.60 mg/L to 73.17 mg/L, respectively. The contents of $Cl^-$, $SO_4^{2-}$ and $HCO_3^-$ varied from 39.39 mg/L to 91.87 mg/L, 90.73 mg/L to 355.41 mg/L and 226.78 mg/L to 315.34 mg/L, respectively. The abundance order of the major ions was $Na^+ > Ca^{2+} > Mg^{2+} > K^+$ and $HCO_3^- > SO_4^{2-} > Cl^-$ for cations and anions, respectively.

As to the shallow phreatic groundwater samples, the pH concentrations varied from 7.30 to 7.70 with an average value of 7.51, implying that the samples were also neutral to slight-alkalinity. The TDS in the groundwater varied between 235.00 mg/L and 353.00 mg/L, suggesting that the samples were categorized into freshwater. According to the mean concentration, the major ions have the same abundance order to the upper confined aquifer.

### Hydrogeochemical facies

The Piper diagram is widely used to depict the hydrogeochemical facies (Ahmed *et al.* 2019; Jayathunga *et al.* 2020). As can be seen from Figure 2, the samples from the shallow phreatic aquifer fell within the Mg-$SO_4$ (two samples), Mg-Cl (two samples), Na-$HCO_3$ (one sample), Na-$SO_4$ (one sample) and Ca-$SO_4$ (one sample) type zone. In the upper confined aquifer, 52% (nine samples), 42% (seven samples), and 6% (one sample) were in the field of Na-$SO_4$, Na-$HCO_3$ and Mg-$HCO_3$, respectively. According to the recharge, runoff, and discharge of groundwater flow field during the water-rock interaction, the typical anion in each seepage section is $HCO_3^-$, $SO_4^{2-}$, and $Cl^-$, respectively (Chen *et al.* 2021; Chotpantarat & Thamrongsrisakul 2021). In this study, the anionic types of the shallow phreatic aquifer were mainly $SO_4^{2-}$ and $Cl^-$, and anionic types of the upper confined aquifer were mainly $SO_4^{2-}$ and $HCO_3^-$. So, it can be inferred that the shallow phreatic aquifer and the upper confined aquifer were situated in the runoff-discharge and recharge-runoff area, respectively.

Meanwhile, the $Cl^-$ dominant type on the anionic triangle indicated that the chlorine can be originated from the dissolution of halite and/or anthropogenic factors (agricultural and industrial activities, etc). However, the study area is utilized as a water resource protection zone for urban water supply; industry, agricultural and other pollution-related economic activities were prohibited, meanwhile, local authority staff also regularly check whether there are water pollution activities. So, anthropogenic inputs of $Cl^-$ will not take place. Therefore, the source of chloride inherently reflects the natural geological attribution.

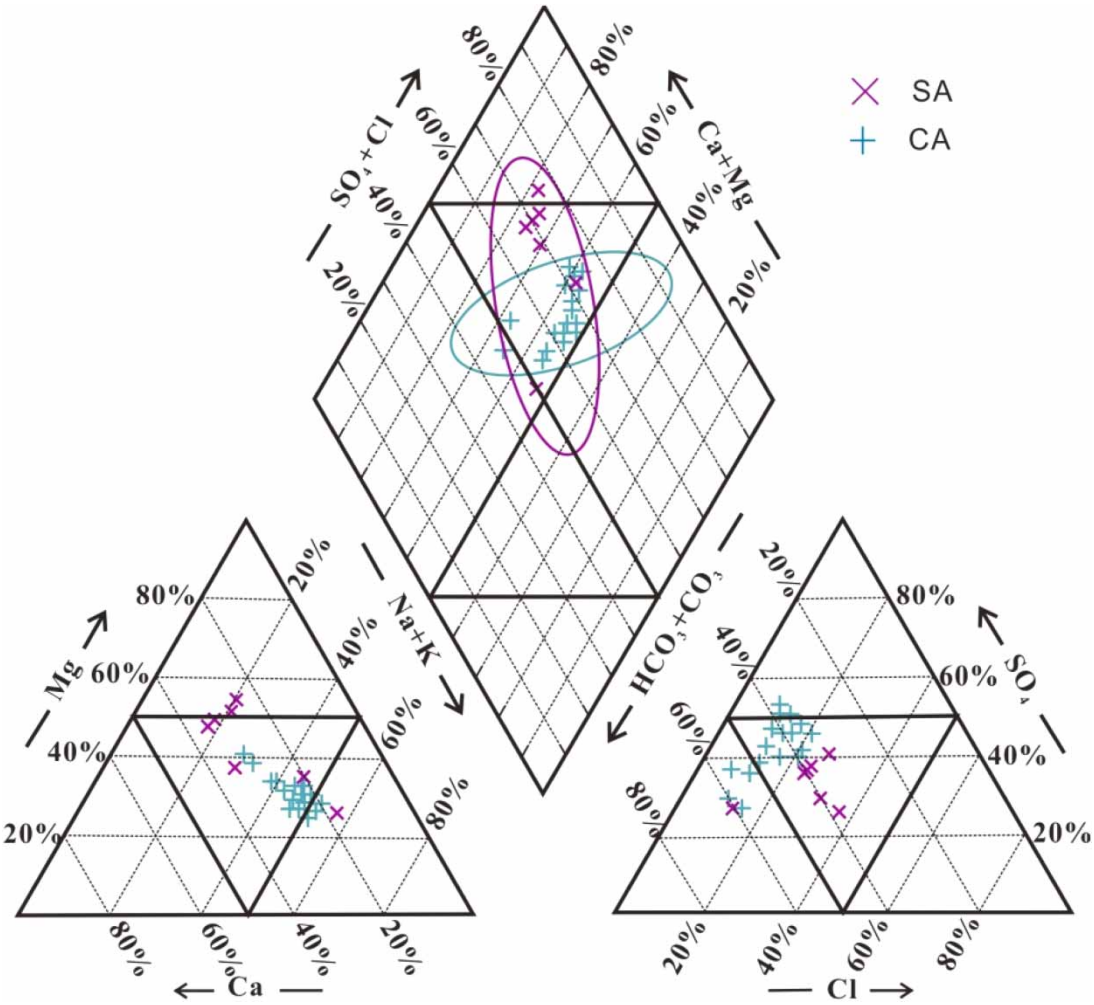


**Figure 2** | Piper diagram of the hydrogeochemical facies.

### Geochemical processes controlling solute sources

The Gibbs diagram, an effective approach for evaluating the source of dissolved chemical constituents, can be used to distinguish the dominant factors controlling the surface water and/or groundwater chemistry, including precipitation dominant, rock dominant (water-rock interaction) and evaporation dominant (Kumar *et al.* 2015; Zaidi *et al.* 2015a, 2015b; Ahmad *et al.* 2019). The ratios of $Cl^-/(Cl^- + HCO_3^-)$ and $(Na^+ + K^+)/(Na^+ + K^+ + Ca^{2+})$ as a function of TDS were plotted in Figure 3. In this study, the shallow aquifer samples and the upper confined aquifer samples were both within the rock dominant area, which indicated that the aquifers were undergoing water-rock interactions.

Major ions ratios are widely applied to proclaim the hydrochemical processes between the aquifer components and groundwater solutes. The scatters falling along the 1:1 line of Na/Cl imply the halite dissolution, the plots above the 1:1 line indicate the ion exchange and/or silicate weathering, and the plots below the 1:1 line suggest reverse ion exchange (Rajmohan & Elango 2004; Touhari *et al.* 2015; Zaidi *et al.* 2015a, 2015b). As seen in Figure 4(a), all the Na/Cl ratios of the confined aquifer were more than 1, suggesting that in addition to halite dissolution, silicate weathering and/or ion exchange may occur in the aquifer. Compared to the confined aquifer, the scatters of the shallow phreatic aquifer fell on both sides of the 1:1 line, suggesting that besides the halite dissolution, the dominant interactions also contained the ion exchange and/or reverse ion exchange and/or silicate weathering. This hydrogeochemical process can be confirmed by the ratio of $(Ca^{2+} + Mg^{2+})/(SO_4^{2-} + HCO_3^-)$. All the $(Ca^{2+} + Mg^{2+})/(SO_4^{2-} + HCO_3^-)$ values of the upper confined aquifer are less than 1 (Figure 4(c)), which also reveals that the primary processes of this aquifer include ion exchange and/or silicate weathering (Paul *et al.* 2019). However, the ratios of $(Ca^{2+} + Mg^{2+})/(SO_4^{2-} + HCO_3^-)$ in the shallow phreatic aquifer scattered on both sides of the 1:1 line, showing carbonate weathering and/or reverse ion exchange may be taking place. Besides, the scatters of $(Ca^{2+} + Mg^{2+}\text{-}HCO_3^-\text{-}SO_4^{2-})/(Na^+ + K^+\text{-}Cl^-)$ supplemented that the confined aquifer was undergoing ion-exchange interaction (Figure 4(d)). Nevertheless, the shallow phreatic aquifer experienced two reactions of ion exchange and reverse ion exchange simultaneously.

Except for few plots of $Ca/SO_4$ scattering along the 1:1 line, indicating the dissolution of gypsum may furnish $Ca^{2+}$ and $SO_4^{2-}$, most $Ca/SO_4$ ratios of two aquifers were less than 1 (Figure 4(b)), which suggested that $SO_4^{2-}$ can be obtained from the dissolution of Glauber's salt and/or ion exchange (Li *et al.* 2016).

### Hydraulic connectivity assessment

Characteristic ion such as $Cl^-$ concentration, stable isotope analysis and multivariate statistic analysis including cluster analysis and discriminant analysis have been employed to determine the hydraulic connectivity between different aquifers (Qian

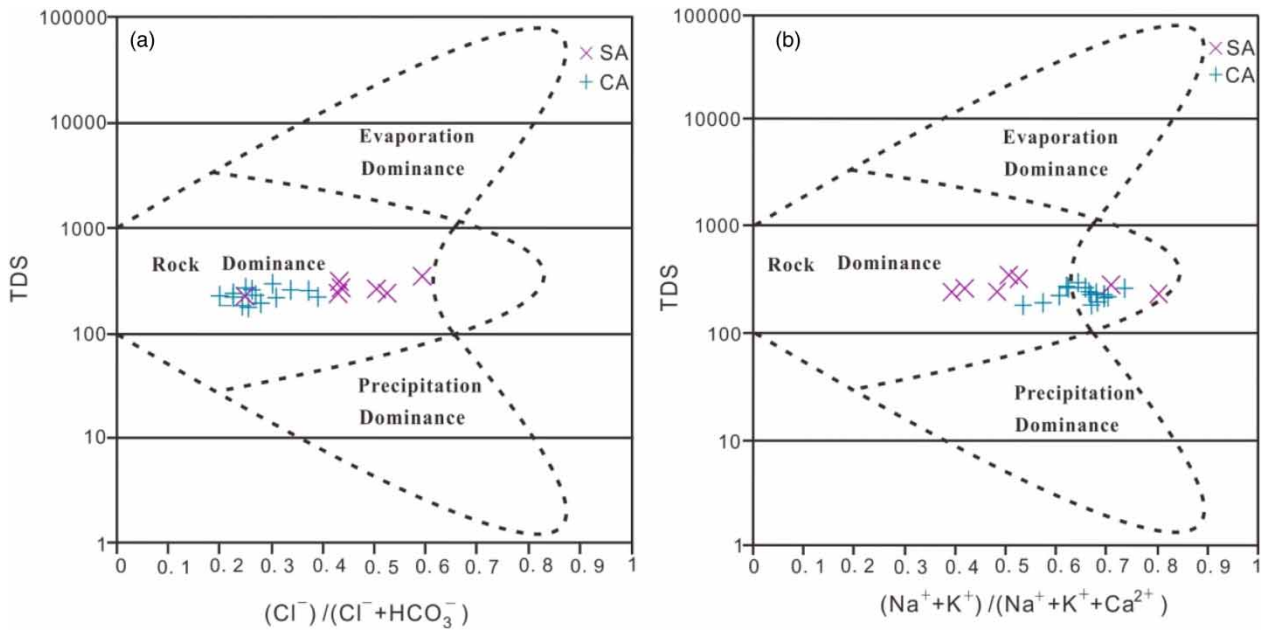


**Figure 3** | Gibbs diagram in the study area.

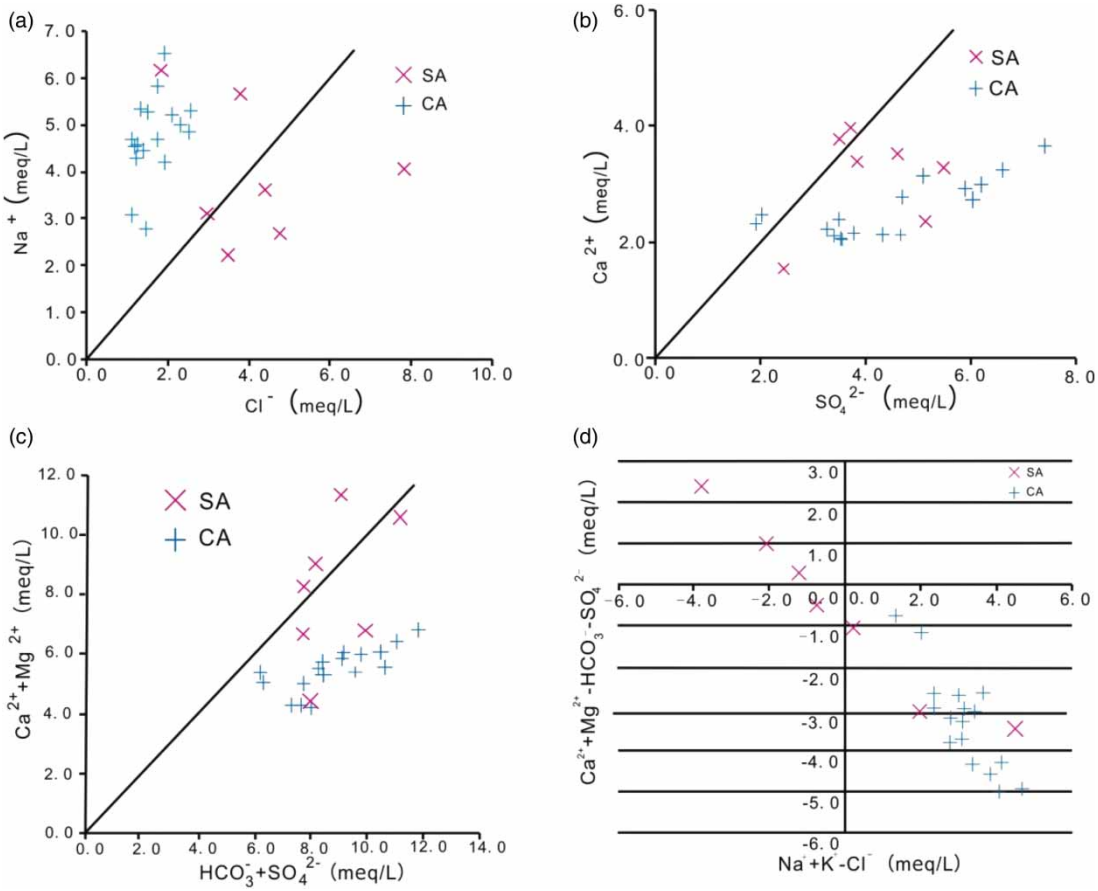


**Figure 4** | Scatter plots of major ions of the two aquifers (SA and CA).

*et al.* 2016; Li *et al.* 2018; Chen *et al.* 2019; Zhang *et al.* 2020). In the present study, $Cl^-$ concentration, stable isotope analysis, and cluster analysis were implemented to master hydraulic connectivity between the shallow phreatic aquifer and the upper confined aquifer.

### Stable isotope analysis

The isotope contents of 7 shallow phreatic aquifer samples and 15 upper confined aquifer samples were listed in Table 2. In the shallow phreatic aquifer, the $\delta^2$H values ranged from −60.47‰ to −49.42‰ with a mean of −53.85 ‰, the $\delta^{18}$O values ranged between −8.08‰ and −6.58‰ with a mean of −7.36‰. The $\delta^2$H and $\delta^{18}$O compositions of the upper confined aquifer varied from −61.89‰ to −55.16‰ with a mean of −58.29‰ and −8.98‰ to −6.94‰ with a mean of −7.83‰, respectively. The global meteoric water line (GMWL) and local meteoric water line (LMWL) were cited as a reference for analyzing the isotope characteristics of the aquifers (Chen & Gui 2021). As shown in Figure 5, all of the samples from the two aquifers were near the GMWL and LMWL, indicating that the precipitation was the major source replenishing the two aquifers. Meanwhile, seven shallow phreatic aquifer samples and fourteen upper confined aquifer samples were located

**Table 2** | The values of hydrogen and oxygen isotopic compositions

| | CA $n = 15$ | | | | SA $n = 7$ | | | |
|---|---|---|---|---|---|---|---|---|
| **Parameters** | **Min** | **Max** | **Mean** | **SD.** | **Min** | **Max** | **Mean** | **SD.** |
| $\delta^{18}$H | −61.89 | −55.16 | −58.29 | 1.87 | −60.47 | −49.42 | −53.85 | 3.72 |
| $\delta^2$ O | −8.98 | −6.94 | −7.83 | 0.48 | −8.08 | −6.58 | −7.36 | 0.57 |

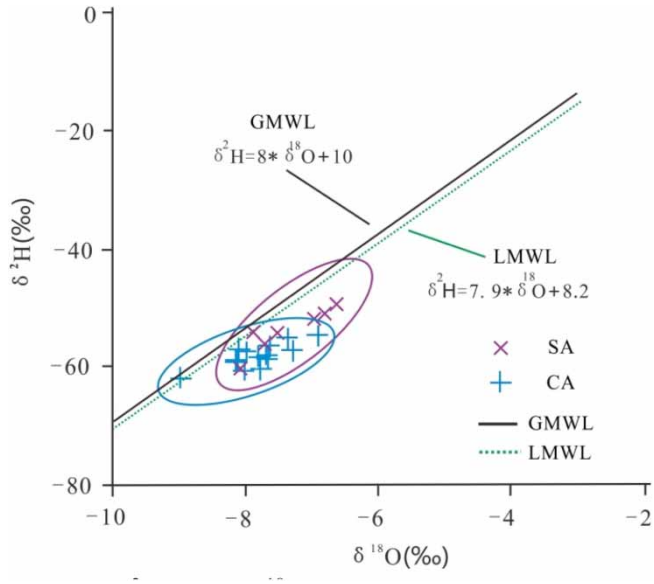


**Figure 5** | $\delta^2$H versus $\delta^{18}$O of SA and CA aquifer samples.

at the lower right of the GMWL and LMWL, reflecting that these samples had been affected by evaporation and showed heavy isotope enrichment. Moreover, there was an overlapping area of two aquifers, which implied that the samples within this area had similar isotope characteristics, and hydraulic connectivity may be happening between these two aquifers.

### Connectivity index assessment

In order to compute the extreme range of the aquifers' connectivity, the minimum, maximum and average values of two aquifers were used to evaluate the variation range of the hydraulic connectivity. As shown in Table 3, the connectivity index values ranged from 0.25 to 2.31, indicating that the connectivity between the two aquifers was between low and moderate. According to the hydrogeolgical condition, hydraulic connectivity may be created between these two aquifers, and the channels of water conservancy connection are mainly lenses formed by lithologic changes.

### Cluster analysis

Based on the Ward method and Euclidean distance, a dendrogram was composed in Figure 6. The results generated two clusters: Cluster I consisted of 1, 2, 3, 4, 5, 6, 8, 9, 10 and 11; cluster II included 7, 12, 13, 14, 15, 16, 17, 18, 19, 20, 21, 22, 23 and 24. Combined with the layout of sampling points (Figure 1), it can be seen that the locations of cluster I were concentrated in

**Table 3** | Connectivity index of the two aquifers

| Aquifer | Cl concentration (mg/L) | | Connectivity index | Gradation |
|---|---|---|---|---|
| SA | Mean | 59.69 | 0.85 | Low |
| CA | Mean | 147.27 | | |
| SA | Min | 65.21 | 0.26 | Moderate |
| CA | Max | 91.87 | | |
| SA | Min | 65.21 | 0.25 | Moderate |
| CA | Min | 39.39 | | |
| SA | Max | 278.11 | 2.31 | Low |
| CA | Min | 39.39 | | |
| SA | Max | 278.11 | 1.8 | Low |
| CA | Max | 91.87 | | |

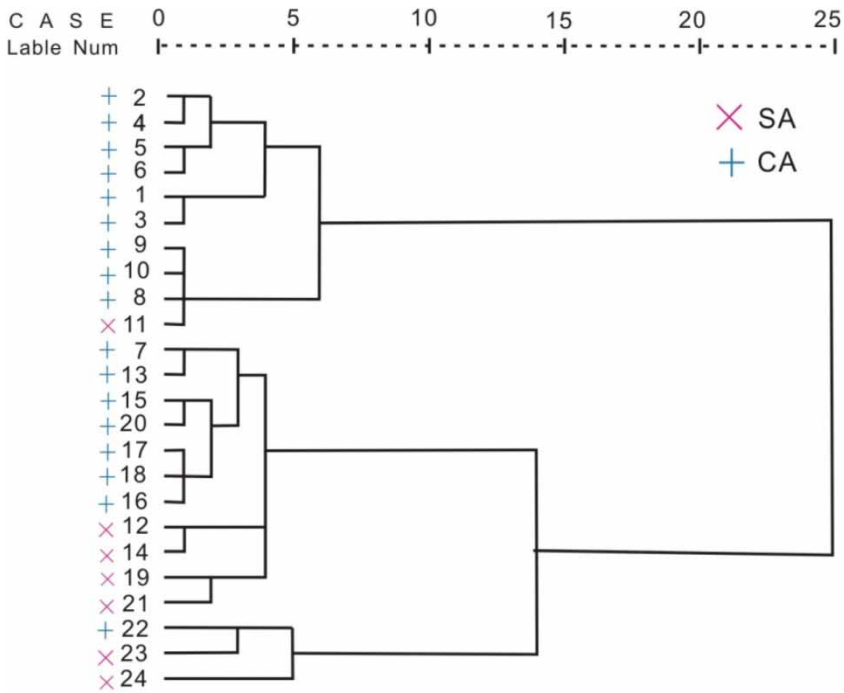


**Figure 6** | Cluster dendrogram of the two aquifer samples.

the west of the study region, which was on the outskirts of the urban area; the locations of cluster II were situated in and around the center of the urban area, in which long-term groundwater abstraction had been conducted by local waterworks. Two cluster areas both emerged hydraulic connectivity between these two aquifers, which further implied that a certain degree of hydraulic connection between the aquifers had been formed.

As mentioned above, the low connectivity implied that, due to the long-term groundwater exploitation, leakage between the adjacent aquifers had probably engendered. The moderate connectivity intimated that the direct water connection between the adjacent aquifers may occur via a water-conducting passageway and/or aquitard thinning zone. The regional hydrogeological exploration can verify this hydraulic condition in and around the center of the urban area, the lenses and/or leakage recharge via the aquitard, confirmed by a large amount of drilling work, can make the two aquifers penetrate each other, resulting in the aquifers' hydraulic connectivity.

## Drinking and irrigation evaluation

### Quality evaluation for drinking purposes

Compared with WHO (2011), it was found that the pH of all the samples were within the standard (6.5–8.5), indicating that all of the samples were well suitable for drinking. The TDS of all the samples were less than 1,000 mg/L, suggesting that the samples were proper for drinking. With respect to the limit concentrations of sodium (200 mg/L), potassium (12 mg/L), magnesium (150 mg/L) and calcium (200 mg/L), none of the samples exceeded the recommended value. For the chloride, only one sample from the shallow aquifer was greater than the limit of 250 mg/L. In regard to sulfate, a total of 71% from the shallow unconfined aquifer and 86% from the confined aquifer were within the limit of 250 mg/L, which were comfortable for drinking. In order to ensure drinking safety for residents, the government had explicitly demonstrated that the groundwater should be treated by waterworks before it can be utilized for drinking water.

### Quality evaluation for irrigation purposes

In the present study, the RSC, SAR and %Na were implemented for the irrigation classification, and the results are shown in Table 4. With respect to the percentage of sodium, which can change the soil structure and affect plant growth, it was observed that five samples accounted for 71% of the phreatic aquifer and two samples accounted for 12% of the upper confined aquifer were suitable for irrigation purposes. Meanwhile, 29% of the phreatic aquifer and 88% of the upper confined

**Table 4** | Classification of the irrigation assessment based on RSC, SAR and %Na

| Paramerers | Range | Water class | Number of the samples | | Percent of the samples (%) | |
|---|---|---|---|---|---|---|
| | | | SA | CA | SA | CA |
| %Na | <20 | Excellent | 0 | 0 | 0 | 0 |
| | 20–40 | Good | 5 | 2 | 71 | 12 |
| | 40–60 | Permissible | 2 | 15 | 29 | 88 |
| | 60–80 | Doubtful | 0 | 0 | 0 | 0 |
| | >80 | Unsuitable | 0 | 0 | 0 | 0 |
| SAR | <10 | Excellent | 7 | 7 | 100 | 100 |
| | 10–18 | Good | 0 | 0 | 0 | 0 |
| | 18–26 | Doubtful | 0 | 0 | 0 | 0 |
| | >26 | Unsuitable | 0 | 0 | 0 | 0 |
| RSC | <1.25 | Good | 7 | 7 | 100 | 100 |
| | 1.25–2.5 | Doubtful | 0 | 0 | 0 | 0 |
| | >2.5 | Unsuitable | 0 | 0 | 0 | 0 |

aquifer were permissible for irrigation, respectively. It revealed that most of the aquifer samples fell in the zone from good to permissible for irrigation.

Residual sodium carbonate (RSC) can influence the suitability for irrigation. A high value of RSC in the groundwater can increase the adsorption of sodium in the soil. The calculated values of RSC ranged from −2.41 meq/L to −0.30 meq/L of the upper confined aquifer and −5.93 meq/L to −1.15 meq/L of the phreatic aquifer, respectively. This indicated that all of the samples were appropriate for irrigation usage, and these waters offered no harm to the plant growth.

Sodium absorption ratio (SAR) is always used as an indicator of adsorption of $Na^+$ in the soil. All of the SAR values were less than 10 meq/L, suggesting that all of the samples were of good quality for irrigation purposes. In addition, the USSL diagram (Figure 7), which was a supplementary method to depict the salinity hazard and alkalinity hazard (Adimalla *et al.* 2018; Li *et al.* 2018), showed that sixteen confined aquifer samples and all the shallow phreatic aquifer samples fell in the C3S1 zone, implying high salinity hazard and low alkalinity hazard. So, when using this groundwater, salt-tolerant plants should be planted preferentially.

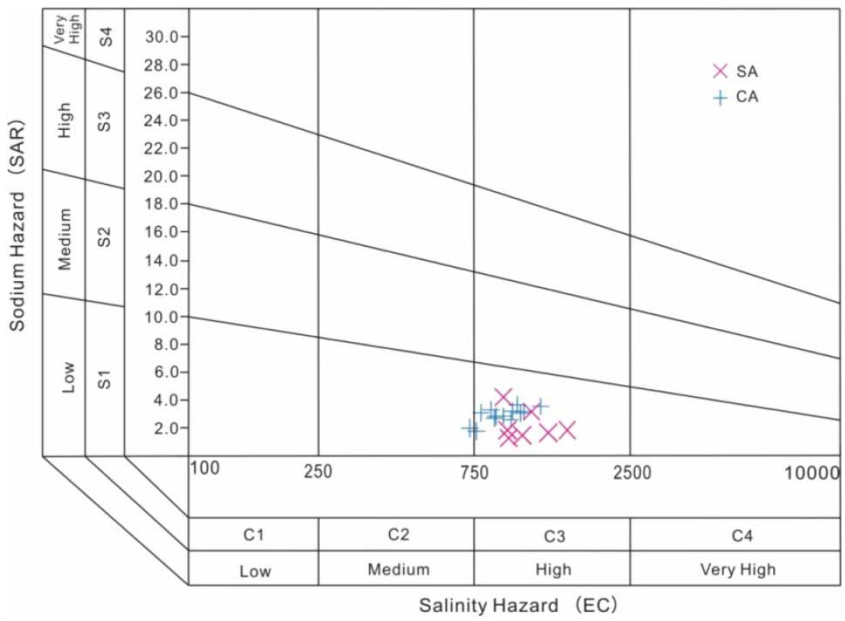


**Figure 7** | USSL diagram for irrigation assessment.

## CONCLUSIONS

Groundwater is the most important water resource for local industry, agriculture, domestic and other activities. In the present study, hydrochemical methods, graphical approaches, connectivity index and statistical analysis were applied to evaluate the hydrochemical processes, groundwater quality, and hydraulic connectivity of these two aquifers. The following conclusions can be drawn:

(1) Both of the two aquifers were neutral to slight-alkalinity and belonged to freshwater. The abundance order of the major ions was $Na^+ > Ca^{2+} > Mg^{2+} > K^+$ and $HCO_3^- > SO_4^{2-} > Cl^-$ for cations and anions, respectively.
(2) The Gibbs diagram indicated that the aquifers were undergoing water-rock interaction, such as halite dissolution, ion exchange, reverse ion exchange, silicate weathering, and followed by the dissolution of Glauber's salt.
(3) The isotope concentrations of SA and CA aquifers suggested that precipitation was the major source replenishing the two aquifers, and most samples has been affected by evaporation and showed heavy isotope enrichment. Similar isotope characteristics implied that hydraulic connectivity had happened between these two aquifers.
(4) Due to the long exploitation of the groundwater, the low connectivity implied that the leakage between the adjacent aquifers had probably engendered. The moderate connectivity intimated that direct water connection between the adjacent aquifers may occur via a water-conducting passageway and/or aquitard thinning zone.
(5) Compared with WHO (2011), the majority of the ion concentration were within the limit for drinking purpose. For the chloride, only one sample from the shallow aquifer are greater than the limit of 250 mg/L. In regard to sulfate, a total of 71% from the shallow unconfined aquifer and 86% from the confined aquifer were within the limit of 250 mg/L.
(6) The SAR, RSC and %Na values revealed that the samples are appropriate for irrigation uses. The USSL diagram showed that sixteen confined aquifer samples and all the shallow phreatic aquifer samples implied high salinity hazard and low alkalinity hazard. So, when using this groundwater, salt-tolerant plants should be planted preferentially.

## ACKNOWLEDGEMENTS

This research was financially supported by the Excellent Top-notch Talents Cultivation Foundation of Colleges and Universities, Anhui Province, China (gxbjZD2020091 and gxgnfx2020106), the Natural Science Projects of Colleges and Universities, An-hui Province, China (KJ2020A0739 and KJ2020A0732), the Demonstration Teaching Organization of Anhui Education Department (416), and the Dual-ability Teaching Team Project of Suzhou University (2020XJSN06).

## DATA AVAILABILITY STATEMENT

All relevant data are included in the paper or its Supplementary Information.

## REFERENCES

Adimalla, N., Li, P. & Venkatayogi, S. 2018 Hydrogeochemical evaluation of groundwater quality for drinking and irrigation purposes and integrated interpretation with water quality index studies. *Environmental Processes* **5**, 363–383.

Ahmad, S., Umar, R. & Arshad, I. 2019 Groundwater quality appraisal and its hydrogeochemical characterization – Mathura City, Western Uttar Pradesh. *Journal of the Geological Society of India* **94**, 611–623.

Ahmed, N., Bodrud-Doza, M., Islam, S. M. D., Choudhry, M. A., Muhib, M. I., Zahid, A., Hossain, S., Moniruzzaman, M., Deb, N. & Bhuiyan, M. A. Q. 2019 Hydrogeochemical evaluation and statistical analysis of groundwater of Sylhet, north-eastern Bangladesh. *Acta Geochimica* **38**, 440–455.

Alkinani, M. & Merkel, B. 2017 Hydrochemical and isotopic investigation of groundwater of Al-Batin alluvial fan aquifer, Southern Iraq. *Environmental Earth Sciences* **76**, 301.

Brindha, K., Pavelic, P., Sotoukee, T., Douangsavanh, D. & Elango, L. 2017 Geochemical characteristics and groundwater quality in the Vientiane Plain, Laos. *Exposure and Health* **9**, 89–104.

Chen, S. & Gui, H. 2021 Calculating groundwater mixing ratios in multi-aquifers based on statistical methods: a case study. *Water Practice & Technology* **16** (2), 621–632.

Chen, Y., Zhu, S. & Xiao, S. 2019 Discussion on controlling factors of hydrogeochemistry and hydraulic connections of groundwater in different mining districts. *Natural Hazards* **99**, 689–704.

Chen, K., Sun, L. & Xu, J. 2021 Statistical analyses of groundwater chemistry in the Qingdong coalmine, northern Anhui province, China: implications for water-rock interaction and water source identification. *Applied Water Science* **11**, 50.

Chotpantarat, S. & Thamrongsrisakul, J. 2021 Natural and anthropogenic factors influencing hydrochemical characteristics and heavy metals in groundwater surrounding a gold mine, Thailand. *Journal of Asian Earth Sciences* **211**, 104692.

Hu, Y., Zhang, F., Niu, Z., Dong, Z., Liu, G. & Gao, J. 2014 Hydro-chemical characteristics of groundwater in centralized drinking water sources and its quality assessment in northern Anhui Province. *Journal of University of Science and Technology of China* **44**, 913–920, 925.

Islam, M. M., Marandi, A., Fatema, S., Zahid, A. & Schüth, C. 2019 The evolution of the groundwater quality in the alluvial aquifers of the south-western part of Bengal Basin, Bangladesh. *Environmental Earth Sciences* **78**, 705.

Jayathunga, K., Diyabalange, S., Frank, A. H., Chandrajith, R. & Barth, J. A. C. 2020 Influences of seawater intrusion and anthropogenic activities on shallow coastal aquifers in Sri Lanka: evidence from hydrogeochemical and stable isotope data. *Environmental Science and Pollution Research* **27**, 23002–23014.

Keshavarzi, M., Baker, A., Kelly, B. F. J. & Andersen, M. S. 2017 River–groundwater connectivity in a karst system, Wellington, New South Wales, Australia. *Hydrogeology Journal* **25**, 557–574.

King, A. C., Raiber, M. & Cox, M. E. 2014 Multivariate statistical analysis of hydrochemical data to assess alluvial aquifer–stream connectivity during drought and flood: Cressbrook Creek, southeast Queensland, Australia. *Hydrogeology Journal* **22**, 481–500.

Kumar, S. K., Logeshkumaran, A., Magesh, N. S., Godson, P. S. & Chandrasekar, N. 2015 Hydro-geochemistry and application of water quality index (WQI) for groundwater quality assessment, Anna Nagar, part of Chennai City, Tamil Nadu, India. *Applied Water Science* **5**, 335–343.

Li, P., Wu, J., Qian, H., Zhang, Y., Yang, N., Jing, L. & Yu, P. 2016 Hydrogeochemical characterization of groundwater in and around a wastewater irrigated forest in the southeastern edge of the Tengger Desert, Northwest China. *Exposure and Health* **8**, 331–348.

Li, P., Wu, J., Tian, R., He, S., He, X., Xue, C. & Zhang, K. 2018 Geochemistry, hydraulic connectivity and quality appraisal of multilayered groundwater in the Hongdunzi Coal Mine, Northwest China. *Mine Water and the Environment* **37**, 222–237.

Liu, J., Zhou, D., Gao, Z., Wang, M., Ma, Y., Zhang, H., Shi, M. & Dong, J. 2019 Hydrochemical characteristics and water quality assessment of groundwater in Qingdao West Coast New District. *Journal of Shandong University of Science and Technology (Nature Science)* **38** (2), 14–24. (in Chinese).

Mengistu, H. A., Demlie, M. B. & Abiye, T. A. 2019 Review: groundwater resource potential and status of groundwater resource development in Ethiopia. *Hydrogeology Journal* **27**, 1051–1065.

Mokadem, N., Hamed, Y., Hfaid, M. & Dhia, H. B. 2015 Hydrogeochemical and isotope evidence of groundwater evolution in El Guettar Oasis area, Southwest Tunisia. *Carbonates and Evaporites* **30**, 417–437.

Othman, A., Sultan, M., Becker, R., Alsefry, S., Alharbi, T., Gebremichael, E., Alharbi, H. & Abdelmohsen, K. 2018 Use of geophysical and remote sensing data for assessment of aquifer depletion and related land deformation. *Surveys in Geophysics* **39**, 543–566.

Paul, R., Brindha, K., Gowrisankar, G., Tan, M. L. & Singh, M. K. 2019 Identifcation of hydrogeochemical processes controlling groundwater quality in Tripura, Northeast India using evaluation indices, GIS, and multivariate statistical methods. *Environmental Earth Sciences* **78**, 470.

Qian, J., Wang, L., Ma, L., Lu, Y., Zhao, W. & Zhang, Y. 2016 Multivariate statistical analysis of water chemistry in evaluating groundwater geochemical evolution and aquifer connectivity near a large coal mine, Anhui, China. *Environmental Earth Sciences* **75**, 747.

Rajmohan, N. & Elango, L. 2004 Identification and evolution of hydrogeochemical processes in the groundwater environment in an area of the Palar and Cheyyar River Basins, Southern India. *Environmental Geology* **46**, 47–61.

Saha, N., Bodrud-Doza, M., Islam, A. R. M. T., Begum, B. A. & Rahman, M. S. 2020 Hydrogeochemical evolution of shallow and deeper aquifers in central Bangladesh: arsenic mobilization process and health risk implications from the potable use of groundwater. *Environmental Earth Sciences* **79**, 477.

Shakhane, T. & Fourie, F. D. 2019 An investigation into structural discretisation as a first-order and pilot framework to understand groundwater–stream water connectivity at a reach scale. *Sustainable Water Resources Management* **5**, 883–900.

Sun, F., Wen, Z., Shu, L., Jing, Y. & Lu, C. 2016 Analysis of groundwater pumping-limit and effect in Chengxi well field in Suzhou City. *Water Resources Protection* **32** (1), 184–189. (in Chinese).

Sun, L. 2015 Hydrochemistry of groundwater from loose layer aquifer system in northern Anhui Province, China: source of major ions and hydrological implications. *Water Practice &Technology* **10** (2), 269–276.

Sun, L. & Gui, H. 2015 Hydro-chemical evolution of groundwater and mixing between aquifers: a statistical approach based on major ions. *Applied Water Science* **5**, 97–104.

Touhari, F., Meddi, M., Mehaiguene, M. & Razack, M. 2015 Hydrogeochemical assessment of the Upper Cheliff groundwater (North West Algeria). *Environmental Earth Sciences* **73**, 3043–3061.

WHO 2011 Guidelines for drinking water quality, 4th edn. World Health Organization, Geneva.

Wu, J., Li, P. & Qian, H. 2015 Hydrochemical characterization of drinking groundwater with special reference to fluoride in an arid area of China and the control of aquifer leakage on its concentrations. *Environmental Earth Sciences* **73**, 8575–8588.

Yang, Z., Huang, P. & Ding, F. 2020 Groundwater hydrogeochemical mechanisms and the connectivity of multilayer aquifers in a coal mining region. *Mine Water and the Environment* **39**, 808–822.

Zaidi, F. K., Kassem, O. M. K., Al-Bassam, A. M. & Al-Humidan, S. 2015a Factors governing groundwater chemistry in paleozoic sedimentary aquifers in an arid environment: a case study from Hail Province in Saudi Arabia. *Arabian Journal for Science and Engineering* **40**, 1977–1985.

Zaidi, F. K., Nazzal, Y., Jafri, M. K., Naeem, M. & Ahmed, I. 2015b Reverse ion exchange as a major process controlling the groundwater chemistry in an arid environment: a case study from northwestern Saudi Arabia. *Environmental Monitoring and Assessment* **187**, 607.

Zaki, S. R., Redwan, M., Masoud, A. M. & Moneim, A. A. 2019 Chemical characteristics and assessment of groundwater quality in Halayieb area, southeastern part of the Eastern Desert, Egypt. *Geosciences Journal* **23**, 149–164.

Zhang, X., He, J., He, B. & Sun, J. 2019 Assessment, formation mechanism, and different source contributions of dissolved salt pollution in the shallow groundwater of Hutuo River alluvial-pluvial fan in the North China Plain. *Environmental Science and Pollution Research* **26**, 35742–35756.

Zhang, H., Xu, G., Chen, X., Mabaire, A., Zhou, J., Zhang, Y., Zhang, G. & Zhu, L. 2020 Groundwater hydrogeochemical processes and the connectivity of multilayer aquifers in a coal mine with karst collapse columns. *Mine Water and the Environment* **39**, 356–368.

First received 11 August 2021; accepted in revised form 7 December 2021. Available online 22 December 2021